

Annual Report for:

**MODELING AND DESIGN FOR REDUCED CROSS TALK IN MIXED SIGNAL ANALOG /
DIGITAL IC PACKAGES FOR WIRELESS APPLICATIONS**

D. P. Neikirk, Guanghan Xu, and Leszek Demkowicz
The University of Texas at Austin

AFOSR Grant No. F49620-96-1-0032

Grant Start Date: 12/31/95

Report Period: December 31, 1995 - September 1, 1996

POC: Professor Dean P. Neikirk
Department of Electrical and Computer Engineering
The University of Texas at Austin, Austin, TX 78712
voice: 512-471-4669; FAX: 512-471-5445
e-mail: neikirk@mail.utexas.edu; WWW: <http://weewave.mer.utexas.edu>

INTRODUCTION AND OBJECTIVES

A critical requirement for the development of low cost, wide-bandwidth telecommunications equipment is the close integration of both digital and analog microelectronic components. The physical interface between an IC and its environment is the IC package, and its performance is severely tested by the high speed and high frequencies encountered in wide-bandwidth systems. Single chip mixed signal ICs that combine directly both high frequency analog and high speed digital sub-sections will require proper electromagnetic understanding of capacitive, inductive, and radiative coupling between components, and their impact on high sensitivity analog sub-circuits.

The overall objective of this work is the development of techniques for the analysis and design of mixed signal packages, especially the impact of inductive cross talk between the digital and analog sections of the IC, and techniques to maintain appropriate RF to RF signal line isolation in low cost IC packages. In wireless personal communication services (PCS) units there are particularly severe constraints on package options, since these applications are typically very cost and form-factor sensitive. Some of the major problems induced by digital to analog and analog to analog cross talk are listed below:

- (1) high speed digital clocks cause severe interference with RF or IF front ends;
- (2) in digital portables, time-division-multiple-access (TDMA) may be used and power on / off cycles happen fairly frequently, causing additional transient noise on the power and ground planes;
- (3) in frequency division duplex systems, high-power transmit signals cause interference with weak receive signals since separation by filters is limited;
- (4) the leakage of the amplifier output to the input may cause the amplifier to oscillate.

Under this program, we are developing and testing electromagnetic modeling techniques that can capture such effects; to achieve this it is critical that the electromagnetic analysis tools *exclude* unnecessary effects, but without requiring "expert" intervention. We are developing inductive extraction processes that use ultra-compact equivalent circuits (consisting of frequency-independent elements) to model frequency dependent skin and proximity effects. Recent accomplishments include a new highly efficient simulation method, the surface ribbon method (SRM), that allows much more rapid simulation to be performed. Typically, computation time can be reduced by about a factor of 2000 compared the conventional model. We are currently preparing user software for transmission line impedance modeling based on the SRM, and expect release in first quarter 1997. We have recently derived a rigorous definition for the "effective internal impedance" used with the surface ribbon method, and will begin investigating its use with the finite element method. This approach should allow significant improvement in computation time for FEM-based electromagnetic simulations of finite conductivity structures. We are also studying internal-to-the-package low pass filter designs for analog power supply to chip; pad / pin arrangements for reduced digital power plane-to-analog coupling, for RF controlled impedance connections, and for increased RF-to-RF signal line isolation. Prototypical wireless communications circuits will be used to determine the impact of digital-to analog interference, and validate the models developed.

ACCOMPLISHMENTS FOR THIS REPORTING PERIOD (12/31/95 - 9/1/96)

MINIMUM SEGMENTATION IN SURFACE RIBBON METHOD FOR SERIES IMPEDANCE CALCULATION

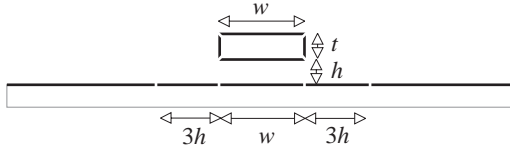
For performance evaluation of integrated circuits accurate characterization of the electrical parameters of various interconnects and packages is essential. As operating speeds and wiring densities increase skin and proximity effects become more important, and cause significant loss and coupling. Various electromagnetic field solvers have been derived to accurately calculate frequency-dependent resistance and inductance, such as the volume filament method (VFM) [1], the finite element method (FEM), the boundary element method (BEM) [2]. However, for

complex two and three dimensional geometries more efficient field solution approaches are desirable. To reduce the number of unknowns and the computational load, non-uniform segmentation schemes, efficient matrix manipulation, and iterative matrix solvers have been developed for the volume filament method [3]. The surface ribbon method (SRM) [4, 5] has also been developed to reduce the problem size using the effective internal impedance (EII) and surface segmentation instead of volume segmentation. In SRM, greater numerical efficiency can be obtained by using minimum number of segments. We have now determined a minimum segmentation scheme for SRM, and have examined the efficiency and accuracy for a wide variety of interconnect geometries, such as a microstrip lines over a finite ground plane and a microstrip line over a meshed ground plane.

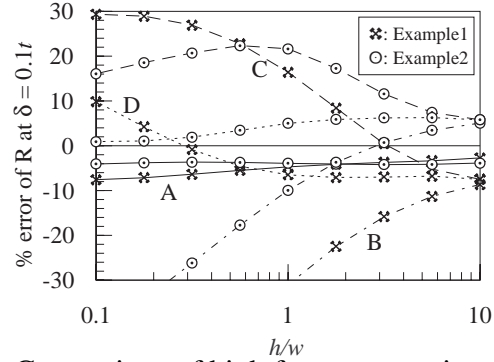
For accurate results at high frequencies, the thickness of a skin depth must be divided into several segments in VFM. Hence, matrix sizes become large, especially at high frequency. To avoid discretizing the conductor interior, the effective internal impedance (EII) can be combined with the current integral equation assuming current flows only at the conductor surface. The method of moments is then applied to this surface current integral equation. The internal behavior of conductor is represented at the conductor surface using an EII and the conductor interior is replaced by the exterior material. Hence, this SRM replaces volume discretization by surface discretization, reducing the number of unknowns, giving fast and accurate results.

Unlike VFM, SRM does not require the use of several segments for the width of a skin depth and, therefore, can significantly reduce the number of unknowns. Figure 1(a) shows a minimum segmentation scheme for the case of a microstrip line over a ground plane. For a signal line with comparable width to thickness ratio, the line can be represented using four segments, one segment for each side of the conductor. In the case of a lossy ground plane, the upper surface of the ground plane must also be discretized. Here we show that only five segments are necessary for accurate results: one segment directly below the signal line with width of w (the width of the signal line), adjacent segments on each side with width of $3h$ (three times the dielectric thickness), and finally one more segment on each side for the remaining ground plane. Therefore, the total number of unknowns becomes nine. This minimum segmentation scheme can be extended to structures having multi-conductors and multi-ground planes.

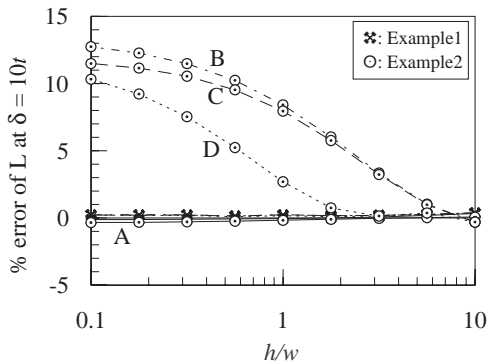
For comparison, we have also considered two other minimum segmentation schemes in SRM. Firstly, a single segment has been assigned to the ground plane. Secondly, the ground plane is discretized into three segments: one segment directly below the signal line with the width of w , and one more segment on each side for the remaining ground plane. Both use four segments for the signal line. For two different microstrip line geometries, resistance and inductance have been calculated using the different segmentation schemes of SRM, as well as with full VFM and a finely divided SRM; example 1 has a signal line 10 μm wide ($w = 10 \mu\text{m}$) and 10 μm thick ($t = 10 \mu\text{m}$), and a ground plane 500 μm wide and 10 μm thick. Example 2 has a signal line of 10 μm wide and 1 μm thick, and a ground plane 500 μm wide and 1 μm thick. Figure 1(b), (c), and (d) compare resistance and inductance as a function of strip height above the ground plane h , from $0.1xw$ to $10xw$ at the low frequency where $\delta = 10t$, and the high frequency where $\delta = 0.1t$. With five segments for the ground plane SRM gives accuracy within 10% for resistance and inductance for both examples. With three segments for the ground SRM deviates by as much as 30% for resistance and inductance. Table 1 shows speed gains of several thousands times compared to VFM and of several ten times compared to SRM using fine segments.



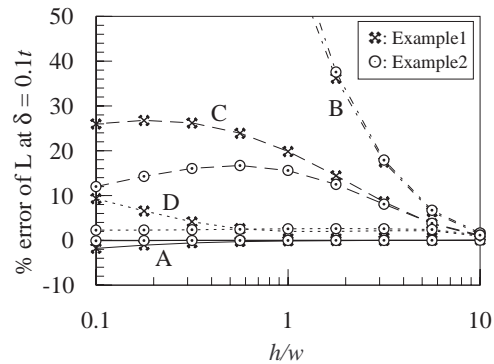
(a) Minimum segmentation scheme for a microstrip line



(b) Comparison of high frequency resistance



(c) Comparison of low frequency inductance



(d) Comparison of high frequency inductance

Figure 1: Minimum segmentation scheme for a microstrip line, and comparison of resistance and inductance calculated using different segmentations in SRM. Resistance and inductance are normalized by the results of VFM. A(solid line): fine segments; B(dot-and-dashed line): one segment for the ground plane; C(dashed line): three segments for the ground plane; D(dotted line): five segments for the ground plane. Minimum segmentations use four segments for the signal line.

Method	Number of unknowns	CPU time[sec]	
		Assembling	Solving per frequency
VFM	660	55.3	100.9
SRM1	120	0.3	0.89
SRM2	9	-	0.012

Table 1: Comparison of run time and the number of unknowns on an IBM RISC 6000 for VFM, SRM, and SRM using minimum segments. Matrix solutions done using simple gaussian elimination.

Similarly, the minimum segmentation scheme can be applied to the three-dimensional surface ribbon method (3DSRM). As an example, the series impedance of a microstrip line obliquely oriented over a meshed ground plane has been calculated, where the signal line is 12 μm wide, 2.5 μm thick and 12 μm over the meshed ground plane of 100x100 μm period with 50x50 μm holes (Fig. 2). In 3DSRM using minimum segments, the signal line is segmented into 3x1 segments with width ratio of 2.8, and an arm of the meshed ground is divided into three segments. For comparison, the partial element equivalent circuit method (PEEC) [6] is also applied, where three different segmentation schemes are used. In PEEC1 the meshed ground is approximated by cascaded straight rectangular bars and divided into 6x3 segments; in PEEC2 an arm of the meshed ground is divided into four segments for wide side and one segment for the thickness; and in

PEEC3 an arm of the meshed ground is divided into four segments for wide side and two segment for the thickness. In PEECs the signal line is divided into non-uniform 12x4 segments. Figure 2 shows the structure and compares resistance and inductance calculated using different schemes. For inductance, PEEC1 is considerably off about 23% from others and 3DSRM gives the result with 5% accuracy. For resistance, PEECs do not capture the skin effect of the ground plane due to coarse segments, and the results deviates more than 20% from the result of 3DSRM. Table 2 compares run time and the number of unknowns of 3DSRM and PEECs.

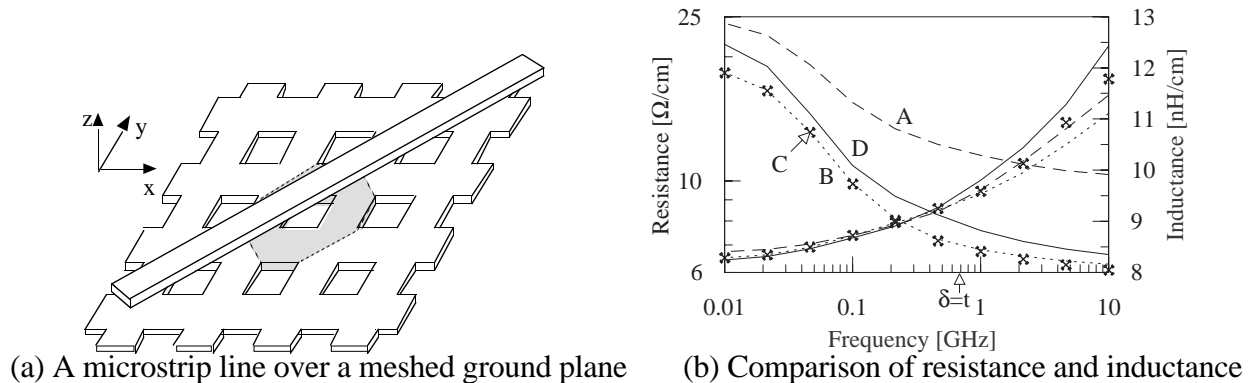


Figure 2: A microstrip line 45° obliquely oriented over a meshed ground plane, and comparison of resistance and inductance between PEECs with three segmentation schemes and 3DSRM. A(dashed line): PEEC with straight line approximation; B(dotted line): PEEC with one layer segment for the ground; C(*): PEEC with two layer segments for the ground; D(solid line) 3DSRM. Meshed ground is considered by 5 apertures perpendicular to the signal line and 9 apertures along the signal line to obtain constant per unit length inductance.

Method	Number of unknowns	CPU time[sec]	
		Assembling*	Solving per frequency
PEEC1	398	1360.1	18.6
PEEC2	283	1788.4	8.0
PEEC3	743	4745.1	146.7
3D SRM	148	37.2	3.1

Table 2: Comparison of run time and number of unknowns on an IBM RISC 6000 for PEECs and 3DSRM. * is in case of 9x5 apertures of the meshed ground. Matrix solutions done using simple gaussian elimination.

COMPACT CIRCUIT LADDERS

Time domain analysis for digital signal propagation requires models covering the entire frequency range from dc to $1/\tau_{\text{rise}}$, where τ_{rise} is the rise time of the signal. For high speed signals with very short rise times, the high frequencies contained in the signal may be high enough that skin effects significantly affect the waveform. The skin effect itself has been extensively studied, although many methods treat the skin effect at high frequencies only, failing to predict the properties of transmission lines at low frequencies. Skin effect lumped circuit models in which the elements are frequency independent have also been used [7-9], but tend to produce very large ladder circuits. Yen *et al.* [9] introduced a more compact circuit model, but this method failed to accurately capture the skin effect at high frequencies and did not establish clear rules governing the choice of component values. We have developed a modification of Yen's method using simple rules for selecting the values of resistors and inductors for a four deep ladder circuit model. The AFOSR Grant No. F49620-96-1-0032

equivalent circuit accurately models the skin effect in circular cross section conductors up to a frequency corresponding to a 100 skin depth radius conductor. We have also developed compact equivalent circuits for the series impedance per unit length for coax and twin lead, including both proximity and skin effects.

For normal lossy transmission lines, since conductor loss increases as frequency increases, for wide bandwidth digital signals the transmission line acts somewhat like a low pass filter. As the signal propagates along the line and high frequency components are attenuated, the effective bandwidth decreases, and hence an "electrically short" length becomes longer. This has been used to reduce the size of lumped ladder models for long transmission lines through the use of non-uniform lumping [10, 11]. This approach can also be used to generate compact circuit models for the skin effect. Yen *et al.* [9] introduced a constant resistance ratio (RR) to try and capture this low pass characteristic. Figure 3 shows a schematic illustration of our compact ladder model.

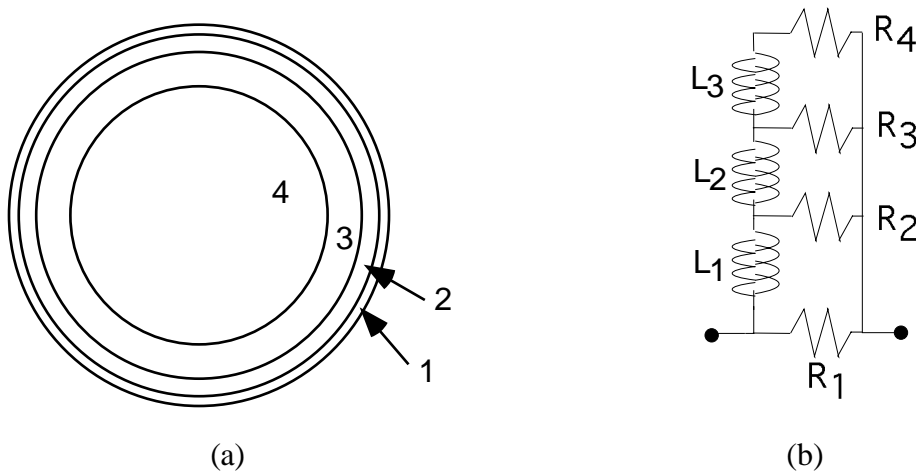


Figure 3: Schematic illustration of four ladder compact circuit model; drawing is to scale for $\alpha_R = 10$, giving $RR = 0.602$.

Here a circular cross section conductor is divided into four concentric rings, each ring represented by one ladder section. For the resistance values each ring is chosen so that $\frac{R_{i+1}}{R_i} = RR$, $i = 1, 2, 3$, where RR is a constant to be determined. We first require that the dc resistance of the ladder be equal to the actual dc resistance of the conductor R_{dc} , and also take the first resistance to be $R_1 = \alpha_R \cdot R_{dc}$. For a four section ladder these two constraints lead to the requirement

$$(RR)^3 + (RR)^2 + RR + (1 - \alpha_R) = 0.$$

Thus, for a given selection of α_R , the resistance ratio RR is fixed by solution of this cubic equation. The inductance values are determined in a similar fashion, with $\frac{L_{i+1}}{L_i} = LL$, $i = 1, 2$, again requiring that the low frequency inductance of the ladder be equal to the actual low frequency internal inductance (L_{lf}) of the wire. Using $L_1 = \frac{1}{\alpha_L} \cdot L_{lf}$ this leads to the constraint that

$$\left(\frac{1}{LL}\right)^2 + \left(1 + \frac{1}{RR}\right)^2 \frac{1}{LL} + \left(\left[\frac{1}{RR}\right]^2 + \frac{1}{RR} + 1\right) - \alpha_L \left(\left[1 + \frac{1}{RR}\right] \left[\left\{\frac{1}{RR}\right\}^2 + 1\right]\right)^2 = 0,$$

This equation can be solved for LL, once RR has been obtained from the solution of the cubic polynomial above and α_L has been selected.

To match the high frequency resistance of the conductor, the resistance of the outermost ring (R_1) is most critical; we have found that if the maximum frequency of interest is ω_{\max} , R_1 should be chosen so that

$$\alpha_R = 0.53 \frac{\text{wire radius}}{\delta_{\max}},$$

where $\delta_{\max} = \sqrt{\frac{2}{\omega_{\max} \mu_o \sigma}}$. To ensure the frequency response from dc to ω_{\max} is well modeled,

we have found that the inductance values must be chosen using $\alpha_L = 0.315 \alpha_R$. Once the dimensions of the conductor and ω_{\max} are specified, all the values of the components in the ladder are fixed, and the response of this circuit from dc to ω_{\max} will match the skin effect. Figure 4 illustrates the advantage of using this method over a uniform lumping method. For instance, over 100 uniform R-L sections are necessary to represent the response of a 50 skin-depth radius circular conductor to similar levels of accuracy as a four section ladder using the procedure discussed above. We have found that for $5 \leq \alpha_R \leq 50$ the local error is not worse than 15%, and with α_R up to 100, the error is still not worse than 25%. This corresponds to wires with radii between about 10 and 100 skin depths at ω_{\max} for less than 15% error, and up to 200 skin depths at 25% error.

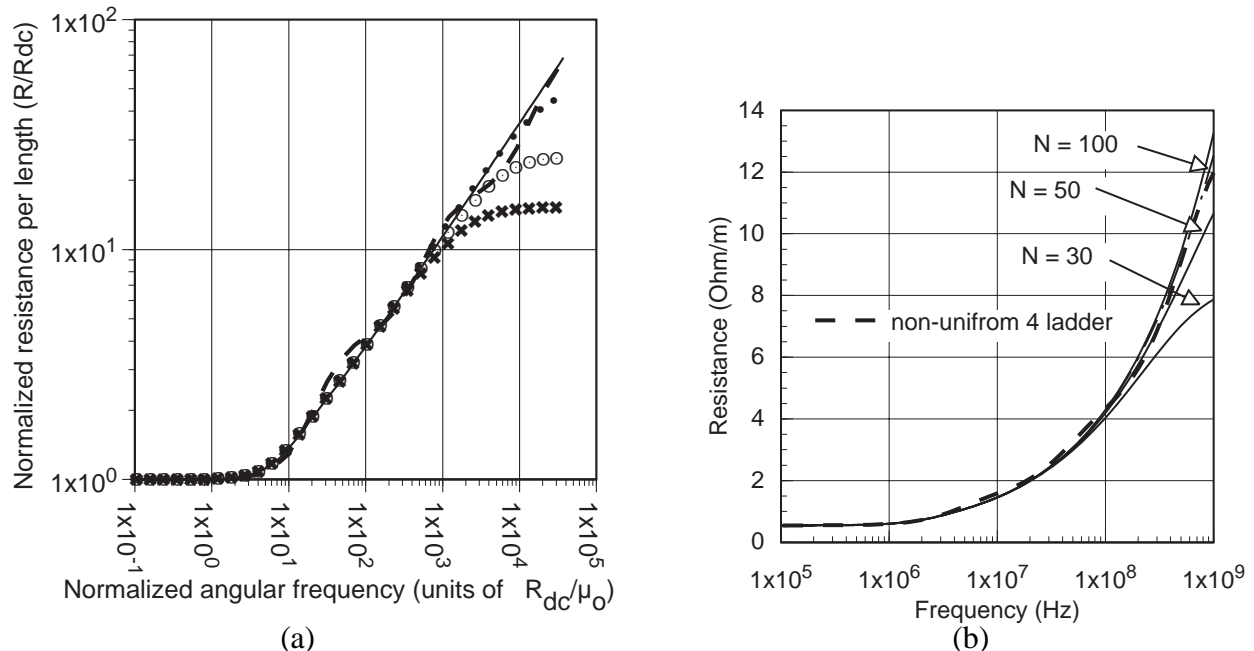


Figure 4: Comparison between uniform lumping and our compact model. N = number of sections used for uniform lumping. Thin line: exact result from solving Helmholtz equation; thick dashed line: four ladder circuit modeling; (a) normalized comparison; • : uniform ladder, 100 sections; ○ : uniform ladder, 50 sections; ✕ : uniform ladder, 30 sections; (b) comparison for copper wire with radius = 0.1 mm.

This approach can be used to model a coaxial line including skin effect in both the center and shield conductors. The exact solution for the series impedance per unit length, including skin effect is [12],

$$Z_{total} = Z_{inside} + Z_{outside} + j\omega L_{ext} = \frac{T}{2\pi\sigma} \left(\frac{1}{a} \frac{J_o(Ta)}{J_1(Ta)} + \frac{1}{b} \frac{J_1(Tc)Y_o(Tb) - J_o(Tb)Y_1(Tc)}{J_1(Tb)Y_1(Tc) - J_1(Tc)Y_1(Tb)} \right) + j\omega \frac{\mu_o}{2\pi} \ln\left(\frac{b}{a}\right)$$

where a is the inner conductor radius, b the inner and c the outer radius of the shield, and $T = \sqrt{-j\omega\mu_o\sigma}$. The series impedance equivalent circuit is shown in Fig. 5a, using the rules presented above applied to both inside and outside conductor, one ladder for the inner conductor using $L_{lf} = \mu_o/8$, and another for the outer shield using [13]

$$L_{lf}^{outer} = \frac{\mu_o}{2\pi} \left[\frac{c^4 \ln(c/b)}{(c^2 - b^2)^2} + \frac{b^2 - 3c^2}{4(c^2 - b^2)} \right].$$

Figure 5b shows the result of circuit modeling for a maximum frequency up to that corresponding to a 100 skin-depth inner conductor radius. Both resistance and inductance are in excellent agreement with the exact results.

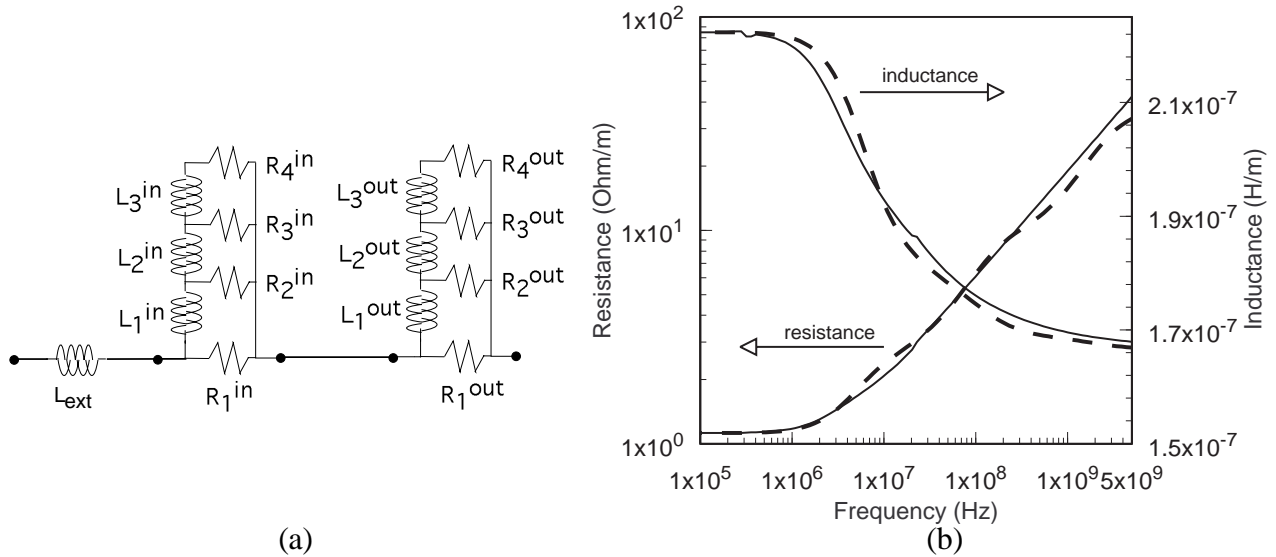


Figure 5: Example of coax line impedance calculation; (a) series impedance skin effect equivalent circuit. (b) Calculated total series impedance for a coaxial line with $a = 0.1$ mm, $b = 0.23$ mm, $c = 0.25$ mm. thin line: exact result; dashed thick line: compact circuit model, $f_{max} = 5$ GHz.

For twin lead, when two conductors are very closely separated both the skin effect, and proximity effect cause series resistance to increase. To approximate the proximity effect with a simple equivalent circuit, we find the fraction of the circular conductor ζ that contributes half the flux at high frequency (Fig. 6a):

$$\zeta = \frac{\theta}{4\pi} = \frac{1}{\pi} \sin^{-1} \left(\sqrt{1 - \left(\frac{r}{d}\right)^2} \right).$$

Two ladders with values determined using the rules presented above are constructed, with one ladder weighted by $1/\zeta$ (representing the inner face of the conductors), the other weighted by

$1/(1 - \zeta)$ (representing the outer faces of the conductors); they are then connected in parallel, as shown in Fig. 6b. Figure 6c shows the equivalent circuit compared to a conformal mapping method [14]. The conformal mapping method over-estimates the low frequency inductance; at low frequencies our circuit model is actually in better agreement with exact results.

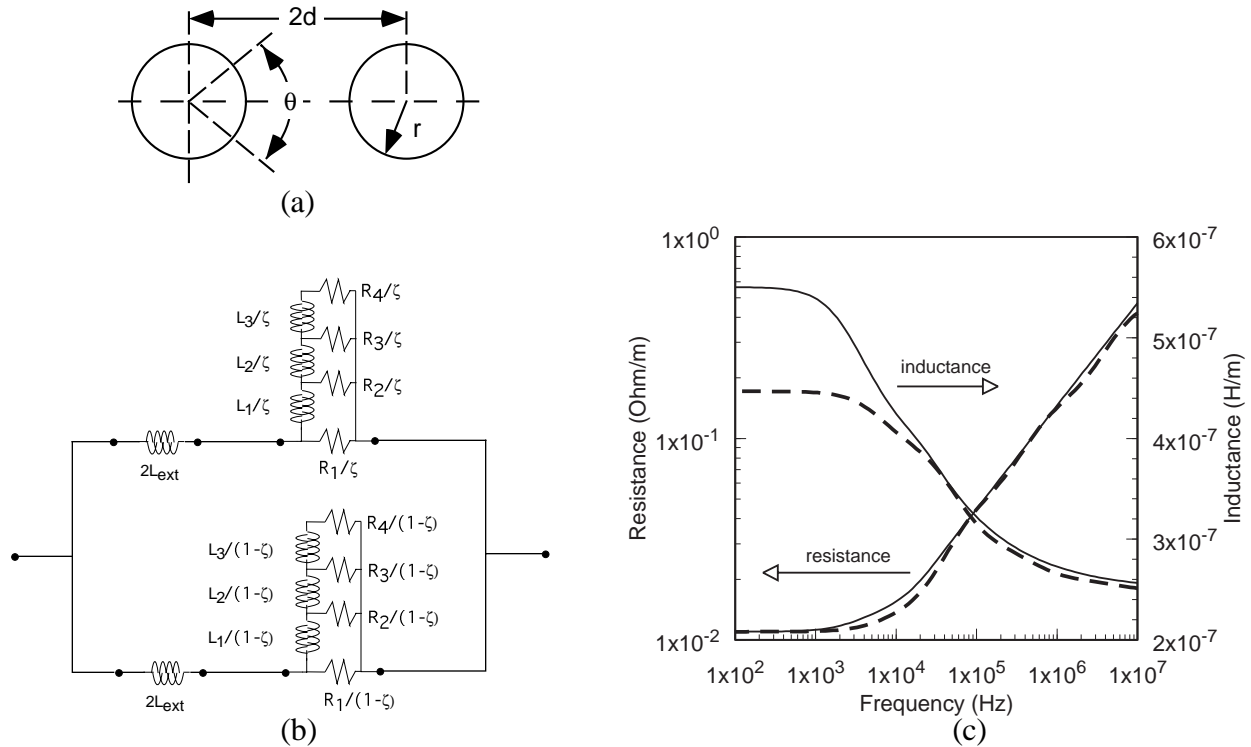


Figure 6: Example of twin lead equivalent circuit including external inductance and the proximity effect. (a) geometry of twin lead; θ represents half the flux coupling the two conductors; (b) equivalent circuit; (c) sample calculation for $r = 1$ mm, $d = 1.2$ mm: thin line: conformal mapping [14]; thick dashed line: circuit model.

HP-FINITE ELEMENTS

Another important advance in the area of computational electromagnetics for application to mixed signal simulation has been in the area the finite element method (FEM). A new *hp*-adaptive technique has recently been validated that allows the local variation of both the element size (h) and the order of approximation (p). This approach has the advantage that complex structures should be easily simulated. The formulation has been demonstrated to allow discontinuous changes in material properties (such as the change from a dielectric to a metal), to be stable, and to easily handle curvilinear geometries. Extensive numerical testing is still required in this area.

SUMMARY AND FUTURE PLANS

In summary, for the period 12/31/95 through 9/1/96, we have extended our ability to efficiently simulate the behavior of realistic interconnects that make use of finite conductivity metals. In particular, we have developed and tested:

- a minimum segmentation scheme for SRM that reduces considerably the amount of computational time required for frequency domain simulation.
- rules for determining a compact circuit model consisting of four resistors and three inductors that accurately predicts the skin effect that can be generalized for application to rectangular conductor geometries and directly applied to time domain calculations.
- initial computational electromagnetics code for FEM simulations.

Work is on-going in all these areas, as well as in construction and testing of actual wireless mixed signal circuits. Future effort in simulations will be focused on time domain simulation, in particular the development of efficient conductor boundary conditions for use in the finite difference time domain (FDTD) method. Future effort in experimental verification will focus on cross talk sources in wireless circuits, especially interference sources with the phase locked loop sections of the analog RF transceiver.

PUBLICATIONS SUPPORTED IN WHOLE OR IN PART BY THIS GRANT DURING THIS REPORTING PERIOD:

S. Kim and D. P. Neikirk, "Compact Equivalent Circuit Model for the Skin Effect," 1996 IEEE-MTT-S International Microwave Symposium, San Francisco, California, June 17-21, 1996, pp. 1815-1818.

REFERENCES

- [1] W. T. Weeks, L. L. Wu, M. F. McAllister, and A. Singh, "Resistive and inductive skin effect in rectangular conductors," *IBM Journal of Research and Development*, vol. 23, pp. 652-660, 1979.
- [2] M. J. Tsuk and J. A. Kong, "A Hybrid Method for the Calculation of the Resistance and Inductance of Transmission Lines with Arbitrary Cross Sections," *IEEE Transactions on Microwave Theory and Techniques*, vol. 39, pp. 1338-1347, 1991.
- [3] M. Kamon, M. J. Tsuk, and J. White, "FASTHENRY: A Multipole-Accelerated 3-D Inductance Extraction Program," *IEEE Transactions on Microwave Theory and Techniques*, vol. 42, pp. 1750-1758, 1994.
- [4] E. Tuncer, B.-T. Lee, and D. P. Neikirk, "Interconnect Series Impedance Determination Using a Surface Ribbon Method," IEEE 3rd Topical Meeting on Electrical Performance of Electronic Packaging, Monterey, CA, Nov. 2-4, 1994, pp. 249-252.
- [5] B.-T. Lee, E. Tuncer, and D. P. Neikirk, "Efficient 3-D Series Impedance Extraction using Effective Internal Impedance," IEEE 4th Topical Meeting on Electrical Performance of Electronic Packaging, Portland, OR, Oct. 2-4, 1995, pp. 220-222.
- [6] A. E. Ruehli, "Equivalent Circuit Models for Three-Dimensional Multiconductor Systems," *IEEE Transactions on Microwave Theory and Techniques*, vol. MTT-22, pp. 216-221, 1974.
- [7] H. A. Wheeler, "Formulas for the skin-effect," *Proceedings of the Institute of Radio Engineers*, vol. 30, pp. 412-424, 1942.
- [8] T. V. Dinh, B. Cabon, and J. Chilo, "New skin-effect equivalent circuit," *Electronic Letters*, vol. 26, pp. 1582-1584, 1990.

- [9] C.-S. Yen, Z. Fazarinc, and R. L. Wheeler, "Time-Domain Skin-Effect Model for Transient Analysis of Lossy Transmission Lines," *Proceedings of the IEEE*, vol. 70, pp. 750-757, 1982.
- [10] T. Dhaene and D. D. Zutter, "Selection of lumped element models for coupled lossy transmission lines," *IEEE Transactions on Computer Aided Design*, vol. 11, pp. 805-815, 1992.
- [11] N. Gopal, E. Tuncer, Dean P. Neikirk, and L. T. Pillage, "Non-uniform lumping models for transmission line analysis," IEEE Topical Meeting on Electrical Performance of Electronic Packaging, Tucson, AZ, 1992, pp. 119-121.
- [12] S. Ramo, J. R. Whinnery, and T. V. Duzer, "Fields and Waves in Communication Electronics," , 2nd ed. New York: Wiley, 1984, p. 181, pp. 181.
- [13] S. Ramo, J. R. Whinnery, and T. V. Duzer, "Fields and Waves in Communication Electronics," , 2nd ed. New York: Wiley, 1984, p. 106, pp. 106.
- [14] E. Tuncer, B.-T. Lee, M. S. Islam, and D. P. Neikirk, "Quasi-Static Conductor Loss Calculations in Transmission Lines using a New Conformal Mapping Technique," *IEEE Transactions on Microwave Theory and Techniques*, vol. 42, pp. 1807-1815, 1994.